**UNIVERSITY OF WATERLOO**
**Faculty of Engineering**
**Nanotechnology Engineering**


Photochemical Studies of Semiconductor Nanoparticles Anchored onto
Graphene Sheets

Prepared by:
Graeme Williams
2B Nanotechnology

**UNIVERSITY OF WATERLOO**
**Faculty of Engineering**
**Nanotechnology Engineering**

Photochemical Studies of Semiconductor Nanoparticles Anchored onto
Graphene Sheets

Radiation Research Building, University of Notre Dame
Notre Dame, Indiana    46556-5674
United State of America

Prepared by:
Graeme Williams
USER ID  g3willia
2B Nanotechnology
May 8, 2008

354 Tallwood Dr.
Orillia, Ontario
L3V 2G9

May 8, 2008

Dr. Marios Ioannidis, director
Nanotechnology Engineering
University of Waterloo
Waterloo, Ontario
N2L 3B9

Dear Sir,

This report, entitled, "Photochemical Studies of Semiconductor Nanoparticles Anchored onto Graphene Sheets," was prepared in fulfillment of the course WKRPT 300 and the work report requirements of my 2B co-op term. This is my third work term report. The purpose of this report is to investigate synthetic methods to anchor Zinc Oxide and Titanium Oxide nanoparticles onto graphene sheets, and to examine their photoelectrochemical properties. This project was completed at the Radiation Laboratory at the University of Notre Dame.

The Radiation Laboratory at the University of Notre Dame is world-renowned in its efforts to produce next-generation solar cell technology. In particular, Dr. Kamat's lab has been fundamental to the development and application of quantum dots, metal and semiconductor nanoparticles and various nanoarchitectures, for the purposes of creating cost-effective solar cells. The lab recently published a paper regarding the potential for a quantum dot rainbow solar cell, which possesses quantum dots of varying sizes decorated on titanium dioxide nanotubes to more efficiently absorb the solar spectrum.

As a member of Dr. Kamat's team, I was responsible for a research project regarding potential applications of graphene sheets to solar cell technology. Carbon nanotubes have been previously examined as a possible conductive framework with which to anchor various nanoparticles. Graphene sheets, which can be considered unrolled carbon nanotubes, provide a unique 2-D framework for many possible applications. In this position, I researched and applied various synthetic methods to create zinc oxide nanoparticle-graphene and titanium dioxide nanoparticle-graphene solutions. I also applied and developed characterization methods to better understand the systems. The successes and failures of the synthetic methods along with the results of the characterization techniques are enclosed in this report.

I hereby confirm that I have received no further help other than what is mentioned above in writing this report. I also confirm this report has not been previously submitted for academic credit at this or any other academic institution. I would like to acknowledge the assistance of Dr. Prashant Kamat for his suggestions and insight into the project. I would also like to thank Brian Seger, David Baker and Kevin Tvrdy for training on equipment and helpful conversations.

Sincerely,

Graeme M. Williams,

# Contributions

The team that I worked for at the Radiation Lab was medium-sized. Dr. Kamat's group is composed of 17 people. I was the sole person working on the graphene sheet-semiconductor nanoparticle project; however, I received assistance from various people in the lab who were working on similar tasks. This assistance included training on various pieces of equipment, suggestions to test and characterize my project and recommendations to improve my results.

The primary goal of Dr. Kamat's group is to design new methods and technology to meet the pending global energy demands. In particular, research is focused on designing and fabricating various nanostructures and nanoarchitectures in order to replace current solar cell technology. These areas of research serve to make solar technology more cost-effective and feasible to implement on a large scale. In order to accomplish this goal, various avenues of research have been addressed, including the use of carbon and semiconductor nanotubes, graphene sheets, metallic and semiconductor nanoparticles and quantum dots. Test systems composed of combinations of these nanostructures typically show unique photoelectrochemical properties, which potentially have applications in solar cell technology.

The primary task that I was responsible for was the creation and the characterization of graphene- and graphene oxide-semiconductor nanoparticle systems. A great deal of effort was made to research previous work in both graphene and semiconductor nanoparticles, and to derive optimal methods of synthesis and characterization. This was completed with the aid of various online scientific journals and suggestions from both Dr. Kamat and graduate students.

The synthesis of graphene oxide was repeated several times at the beginning of the semester in order to attain a sufficient amount of product for future studies. I was responsible to perform basic organic chemistry in this experiment. The oxidation of graphite powder was completed with the use of heavily-oxidizing agents and strong acids. The product was then filtered and dried. The synthesis of the semiconductor nanoparticles required less-intensive procedures that will be discussed further in the report.

The characterization of the graphene oxide-semiconductor nanoparticle systems occupied the majority of my co-op term. In order to better understand the properties of these systems, a number of spectroscopic and microscopic approaches were used with equipment that will be discussed in greater

detail below. While working with graduate students in the lab, I also learned the basics of various photocurrent measurements and I was exposed to Inductively Coupled Plasma spectrometry and X-Ray Diffraction analysis.

Scanning and transmission electron microscopy were initially used to visualize the zinc oxide nanoparticles deposited on the graphene oxide sheets. I was formally trained to use the field emission scanning electron microscope in the Engineering Department. As such, I was responsible for sample preparation, loading and unloading the sample, and varying the conditions, lenses and apertures to attain proper images. Although I was not trained on the transmission electron microscope, I completed my own sample preparation and had the opportunity to adjust several aspects of the microscope and view different areas of my sample. Furthermore, I used the energy dispersive x-ray spectroscopy addition on the transmission electron microscope in order to confirm the presence of the zinc oxide nanoparticles for my research project.

An alternative, more-effective approach to visualize the graphene oxide-semiconductor nanoparticle systems involved the use of atomic force microscopy. This form of microscopy was used to characterize both the zinc oxide and titanium dioxide nanoparticle-graphene oxide systems. I received training to use the tapping mode of the atomic force microscope. In this role, I was responsible for sample preparation, loading my sample and varying the conditions of the microscope in order to obtain proper images. Furthermore, I gained experience in the analysis of images in order to accurately determine graphene oxide sheet and nanoparticle heights.

The semiconductor nanoparticles examined in this report exhibit numerous absorption properties that were analyzed extensively with the UV-Visible spectrometer. UV-Visible spectroscopy is one of the most critical tools in any solar technology lab, as it provides a measurement of the amount of light and the wavelength of light absorbed by a sample.

In contrast to the UV-Visible spectrometer, the spectrofluorometer provides a measurement of the amount and wavelength of light that a sample emits. Fluorescent dyes, quantum dots and various other materials photoluminesce naturally. Throughout this term, I was concerned with the fluorescent property of zinc oxide nanoparticles, which emit a green colour when irradiated with UV light. In addition, the fluorescence lifetime machine was used to determine the average lifetime of the excited zinc-oxide nanoparticles. I received training and conducted experiments on both of these pieces of equipment throughout the term.

Further studies on the research project were made with resistivity tests, thermogravimetric analysis and nuclear magnetic resonance spectroscopy. Resistivity tests were performed using two methods, involving both a liquid-based and a solid-state approach. Both methods were developed by a graduate student and me; however, only the solid-state approach was used to collect data. TGA was completed with the assistance of a graduate student in order to determine differences in the graphene and graphene oxide structure. NMR was performed with the aid of a different graduate student in order to further determine differences in the graphene and graphene oxide structure. In this role, I witnessed the operation of the NMR machine and I was responsible for sample preparation and subsequent analysis of the data.

This report is a direct result of my experiences and efforts on the aforementioned research project. It outlines both the methodologies and the results from the various experiments that I performed on the graphene oxide-semiconductor nanoparticle systems. This project was a significant benefit to my development as an engineer, as it provided first-hand experience in a research-driven environment. In this academic atmosphere, I learned to more-effectively apply the knowledge gained from past courses and previous studies to my work. Furthermore, the research provided experience with nanoscale systems directly related to my field of interest. This term also gave me experience with a large number of pieces of equipment, materials and chemicals.

Graphene systems are a fairly new and unstudied realm of nanotechnology. This research and report were established as a base of understanding, especially with regard to the interaction of various nanoparticles with the 2-D carbon architecture. As such, the results found in this report serve to broaden the knowledge of graphene systems for future applications in the lab. Examples of such applications include the use of 2-D graphene-semiconductor nanoparticle structures for dye- or quantum dot-sensitized solar cells. The graphene oxide-semiconductor nanoparticle systems may also have merit in selective reduction of graphene oxide through excitation of semiconductor nanoparticles at varying lengths of time. Furthermore, they may also be applied to gas-sensing applications or aiding in the dispersion of metal catalysts for fuel cell applications.

# Summary

Two main topics have been addressed in this report. The first objective of this report is to study the photochemical properties of graphene- and graphene oxide-semiconductor systems in order to test their viability as conductive frameworks in next-generation solar cells. In order to accomplish this task, the syntheses of the nanomaterials were examined, and the combined systems were characterized through a variety of spectroscopic, microscopic and analytical techniques. The second aspect of the report is a development of the first topic. It involves the unique characteristic of semiconductor nanoparticles to photocatalytically reduce graphene oxide. This trait was studied extensively and explored using many different characterization techniques.

This report includes a brief introduction into solar cell technology and motivation for the subsequent research. The report then explains the synthetic methods and unique photochemical properties of the materials of interest: graphene/graphene oxide, zinc oxide nanoparticles and titanium dioxide nanoparticles. The following sections of the report are dedicated to the characterization of the systems, with relations to potential applications and suggestions for areas of further research.

The primary conclusions of this report are that graphene oxide and graphene serve as effective frameworks with which to anchor semiconductor nanoparticles. Graphene oxide and graphene serve to quench zinc oxide nanoparticle fluorescence, indicating an electron transfer from the excited nanoparticle to the 2-D carbon-oxygen sheets. In addition, it has been shown that semiconductor nanoparticles may partially reduce the graphene oxide sheets to a more conductive form through the partial removal and rearrangement of functional groups.

The major recommendations of this report focus on the need to further characterize and further study these systems. Suggested areas of research and refinement include developing better resistivity measurement techniques, better-characterizing the graphite oxide preparation methods, understanding the electron storage effect of graphene and probing the functional groups of graphene oxide through Fourier Transform Infrared Spectroscopy. It is also recommended that additional semiconductor nanoparticles are anchored onto the graphene oxide sheets in order to better understand the photocatalytic reduction mechanism. Further, it would be interesting to explore the properties of sensitizer-semiconductor nanoparticle-graphene oxide systems.

## Conclusions

From the analysis in the report body, it was concluded that:

- Both zinc oxide and titanium dioxide nanoparticles readily adsorb onto the graphene oxide and reduced graphene oxide sheets through Van der Waals and electrostatic forces
- Graphene oxide and reduced graphene oxide have the capacity to quench zinc oxide nanoparticle fluorescence through electron transfer mechanisms, with reduced graphene more strongly quenching the fluorescence
- Semiconductor nanoparticles with sufficient band gap energy can partially reduce graphene oxide through electron transfer from the photoexcited nanoparticles to the graphene oxide sheets
- Reduction of graphene oxide to graphene can be seen as a change in colour from brown to black, which can be quantified through absorption measurements
- Approximately 50% of the oxygen groups in graphene oxide may potentially receive an electron from the excited semiconductor nanoparticles in order to undergo reduction
- The photocatalytic reduction of graphene results in an order of magnitude decrease in resistivity
- The photocatalytic reduction mechanism of graphene oxide results in the rearrangement, but not necessarily the elimination, of the functional groups

# Recommendations

Based on the analysis and conclusions in this report, it is recommended that:

- Further characterization is performed on the graphite oxide and graphene oxide materials, and more definitive synthesis techniques are developed

- Methods are used to better understand the electron storage effect of graphene and graphene oxide, and potential applications of this storage effect are also explored

- The resistance measurements of the graphene oxide and reduced graphene oxide are confirmed through additional techniques (such as spin coating the graphene oxide solution and application of gold evaporation techniques to make electrical contacts)
  - The measured values through this method should also be translated into conductivity values in order to better compare to the values to literature

- The functional groups on the graphene oxide and reduced graphene oxide are further probed through Fourier Transform Infrared Spectroscopy

- Different graphene oxide-semiconductor nanoparticle systems are examined, including both higher and lower energy band gap semiconductor materials

- Graphene oxide-semiconductor nanoparticle-sensitizer systems are examined in order to better understand the electron transfer mechanism and further examine the feasibility of graphene for its role in sensitized solar cells

# Table of Contents

# List of Figures

# List of Tables

# 1. Introduction

The intent of this report is to discuss the synthesis and characterization of graphene oxide (GO)-semiconductor nanoparticle systems. In particular, zinc oxide (ZnO) and titanium dioxide (TiO$_2$) nanoparticles have been chosen to be analyzed in this study, as they exhibit unique fluorescent and absorption properties respectively [1], [2], [3], [4]. These properties have been utilized to provide insight into the interactions between the GO sheets and the attached nanoparticles.

Graphene and GO sheets are relatively unstudied with regard to the field of photochemistry and photovoltaic devices. Graphene sheets are analogous to unrolled, 2-D carbon nanotubes. They are individual sheets taken from the large, stacked-sheet structure of graphite. The carbon sp$^2$ network of single- and bilayer-graphene exhibits unique 2-D electronic transport that has been shown to give strong conductivity [5]. Given the potentially cheap cost of graphene, there is a significant drive within the scientific community to gain a greater understanding of its properties and its possible applications. In the past year, the potential for conductive graphene-based paper [6], and transparent graphene-based conductive electrodes have been explored [7].

Large band gap materials such as zinc oxide and titanium dioxide nanoparticles may have applications in dye- and quantum dot-sensitized solar cells when deposited on graphene sheets. ZnO and TiO$_2$ nanoparticles have been previously examined in combination with carbon nanotubes, showing an electron accepting and storing capacity of the nanotubes [8], [9]. It is shown in this report that GO sheets may play a similar role, while offering unique 2-D architecture. This report also examines the unique ability of semiconductor nanoparticles to partially reduce GO samples when excited with UV light.

In order to understand this report, it is expected that the reader understands semiconductor band theory, and has a basic comprehension of microscopy and spectroscopic characterization techniques. The writing herein will provide a brief overview of solar cell technology in order to present a basis and motivation for the research. The report will then focus more extensively on the methods of synthesis and characterization of the ZnO- and TiO$_2$-GO systems. Further characterization of the reduced graphene oxide systems will also be discussed at depth. Characterization techniques will be described throughout the report, and the results of the techniques will be analyzed both qualitatively and quantitatively. Recommendations on areas of further interest and research will also be provided throughout the report.

## 2. Solar Cell Technology and the Potential Role of Graphene Systems

Rising oil prices and increasing energy demands have shifted the focus on the global energy supply to alternate, renewable sources of energy. While various routes of energy supply have been examined, only solar energy has the potential to meet the rising energy demands in the foreseeable future [10]. Current methods of solar technology focus on silicon-based devices for charge separation; however, the application of nanomaterials and nanoarchitectures are being examined to potentially provide cheaper and more effective solar energy conversion.

The most simplistic model of a solar cell involves a material that accepts light (known as the sensitizer) in order to promote an electron to a higher energy state, denoted as the conduction band in semiconductor materials. This electron is then transferred to a conductive framework attached to the anode, which carries the electron through a circuit in order to perform work. The hole created in the original material is scavenged by an electrolyte solution within the cell. Furthermore, the electron is carried to the cathode in the cell, where it regenerates the electrolyte solution. A model of this process, following the progress of the photogenerated electron, is shown below in Figure 1.
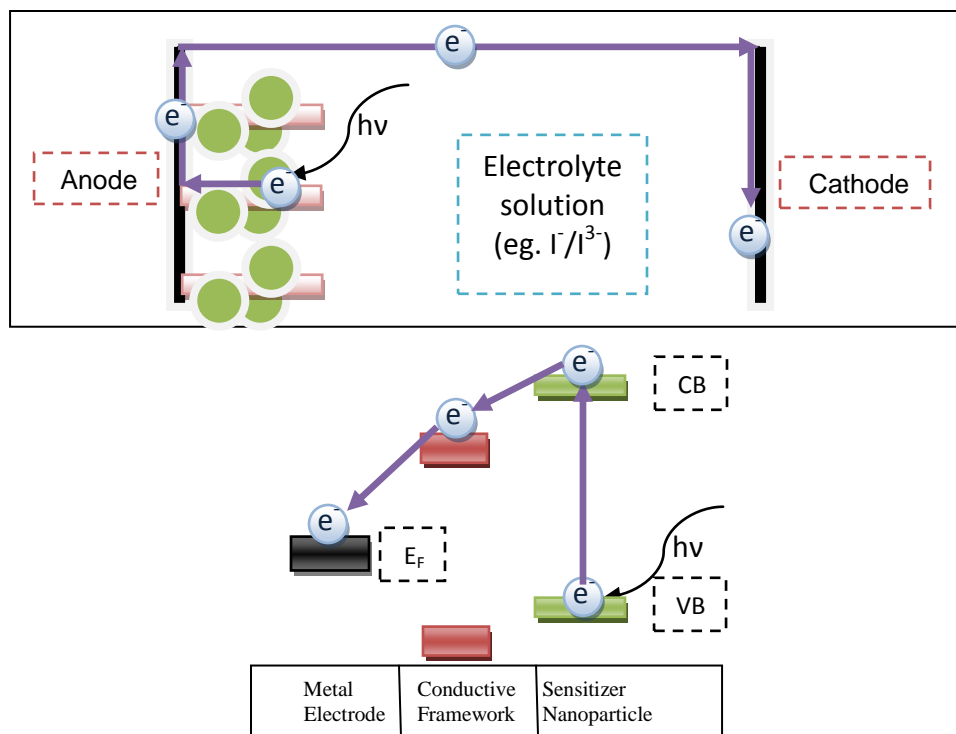


**Figure 1 – A Simplistic Model of a Sensitized Solar Cell**

This report provides a discussion of the properties of graphene and graphene oxide. In the model presented in Figure 1, graphene may potentially play a role as a cheap and effective conductive

framework with which to anchor sensitizer molecules or particles. The unique 2-D transport of the sheets, combined with the low costs of producing graphite and graphene structures, may make it the optimal choice for this application. Furthermore, given the large surface area of graphene sheets, graphene may also serve to disperse the sensitizer molecules and particles in order to achieve greater efficiency. Its large surface area may also have applications in dispersing catalysts for fuel cells.

The synthesis and properties of graphene oxide-semiconductor nanoparticle systems are explored at depth throughout this report. It will be shown that semiconductor particles may be used as a possible means to partially reduce the graphene oxide sheets. This results in a decrease in the resistivity of the sheets. In addition to this application, semiconductor nanoparticles may also be useful to provide a cascading, energetically-favourable pathway for the electrons. More specifically, instead of transferring immediately to the graphene sheets, an electron from a sensitizer may first transfer to a semiconductor nanoparticle and then transfer to the conductive graphene sheets. The transfer to the semiconductor nanoparticle is fast, favourable and hinders recombination of the generated electron and hole in the sensitizer. The energy band diagram for this transition would look similar to the image given in Figure 2.
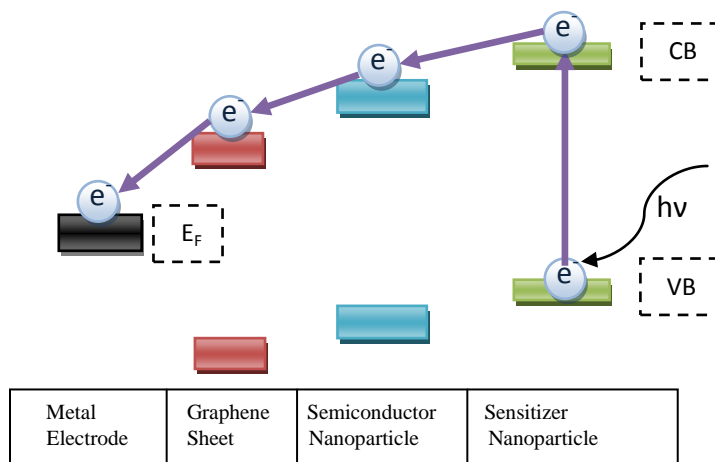


**Figure 2 – Energy Band Diagram for a Sensitized, Semiconductor-Graphene Solar Cell**

# 3. Synthesis and Basic Properties of the Samples of Interest

## 3.1. Graphite Oxide and Graphene Oxide

Although graphite and graphite oxide have been studied for the past century [11], it is only recently that graphene and graphene oxide sheets have been prepared and characterized extensively. In fact, the recent focus on graphene sheets can be attributed to the simple 'micromechanical cleavage' of graphite, where a piece of 'Scotch' tape was used to remove individual sheets of graphene [12]. The most significant challenge in the preparation of graphene is overcoming the strong exfoliation energy of the π-stacked graphene layers in graphite. Micrographitic powder itself cannot be readily separated into individual sheets or dispersed in solvent. Several methods of preparation of graphene and graphene oxide include: oxidation of graphite combined with thermal exfoliation [13], treatment of graphite fluorides with alkyl lithium reagents [14], and oxidation of graphite followed by sonication [15]. The latter method was chosen for all experiments conducted in this study.

Graphite oxide was created using Hummers' method [11], where micrographitic powder was mixed with strongly-oxidizing agents, filtered and dried. The oxidation process functionalizes the graphene sheets with various hydroxyl and epoxy groups, in addition to carbonyl and carboxyl groups along the edges of the sheets. The dried product was suspended in ethanol and sonicated in order to produce disperse, GO sheets. A scheme for this reaction is given below in Figure 3. Further alterations to the original Hummers' method of preparation are available in **Appendix A**. For future studies, it is recommended that solubility, mass composition and in-depth atomic force microscopy (AFM) studies are performed on the GO in order to better distinguish the product. By developing an effective, fully-studied synthesis of graphite oxide, future experiments with graphene will have a stronger basis for characterization.
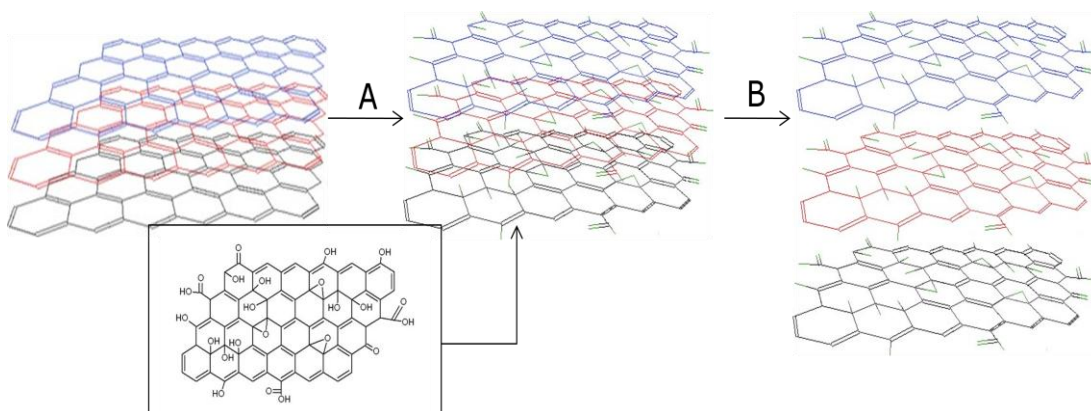


**Figure 3 – Reaction Scheme for the Preparation of Graphene Oxide**

*A: Oxidation of graphite was completed by the addition of micrographitic powder to a concentrated sulfuric acid and sodium nitrate solution, followed by the addition of potassium permanganate and hydrogen peroxide. The solid product was filtered and dried to produce a stable, brown powder. A full description of the experimental procedure is given in Appendix A.*

*B: Exfoliation of the graphene oxide was completed by suspending the graphite oxide powder in ethanol and sonicating the solution for 30 minutes.*
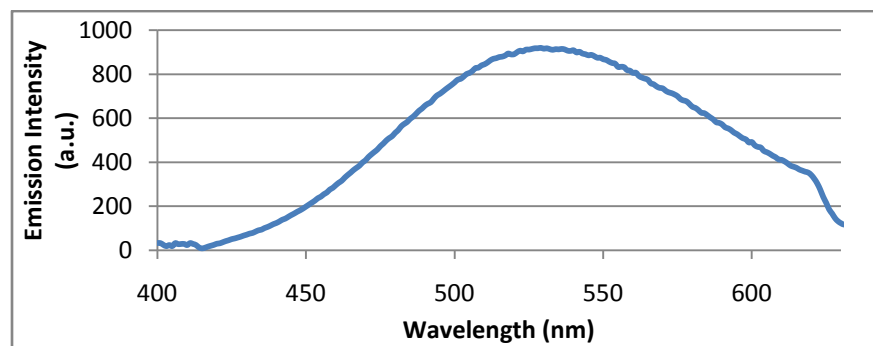
## 3.2. Zinc Oxide Nanoparticles

The method of synthesis for zinc oxide nanoparticles, adopted from literature [8], involved the addition of zinc acetate to an ethanol solution, followed by sonication in an ice bath. Lithium hydroxide was then added to solution and the reaction vessel was further sonicated at room temperature, allowing the particles to grow. A more thorough description of the experimental procedure and pH-related stability issues can be found in **Appendix A**.

Bulk ZnO offers a wide direct band gap of 3.37 eV at 298 K. Using equation (**1**) below, this corresponds to an absorption onset of approximately 368 nm in the electromagnetic spectrum.

$$\lambda \text{ (in nm)} = \frac{hc}{q} \cdot \frac{1}{E \text{ (in eV)}} \cdot 10^9 \tag{1}$$

However, since the method of preparation creates very small particles, size quantization effects result in a slight hypsochromic shift. Immediately after creation, the nanoparticles exhibit an absorption onset at approximately 315nm and eventually absorb at the bulk value of approximately 368nm [8].

ZnO nanoparticles exhibit several unique characteristics when placed under UV light corresponding to the ZnO band gap energy. The most notable characteristic is the capacity for the ZnO nanoparticles to fluoresce green at an approximate peak wavelength of 530nm. The ZnO nanoparticles exhibit a broad fluorescence peak, as illustrated in Figure 4 below.



**Figure 4 – Fluorescence Spectrum of 1 mM ZnO Nanoparticles**

### 3.3. Titanium Dioxide Nanoparticles

$TiO_2$ nanoparticles were created by the hydrolysis of titanium isopropoxide, through the drop-wise addition of titanium isopropoxide to vigorously-stirred ethanol solution [1]. The solutions of colloidal $TiO_2$ were kept under constant stirring in order to prevent agglomeration of the semiconductor nanoparticles. The nanoparticles could be stored indefinitely while stirred. Further specifics on the experimental procedure can be found in **Appendix A.**

Similar to ZnO nanoparticles, the anticipated absorption onset for $TiO_2$ can be calculated for the bulk material using the band gap energy of 3-3.2 eV. Applying equation (**1**), the absorption onset ranges from 388nm to 413nm, depending on the crystal structure of the material. The $TiO_2$ nanoparticles in this study grow to a final absorption onset around 370-375nm, smaller than the bulk material due to size quantization effects.

Excited electrons in the $TiO_2$ nanoparticles can become trapped due to the presence of oxygen vacancies and point defects. The presence of trapped electrons results in the creation of a broad absorption band at approximately 650nm. This additional band causes the $TiO_2$ nanoparticle solution to appear bluish in colour. The evolution of this absorption band can be seen in Figure 1 below. The solution was degassed for approximately 2 minutes per mL of volume and exposed to a Xenon lamp with a water filter at 9 mA. The inert gas is required to observe this band, as oxygen acts as an electron scavenger and would effectively remove excited electrons as they are trapped.
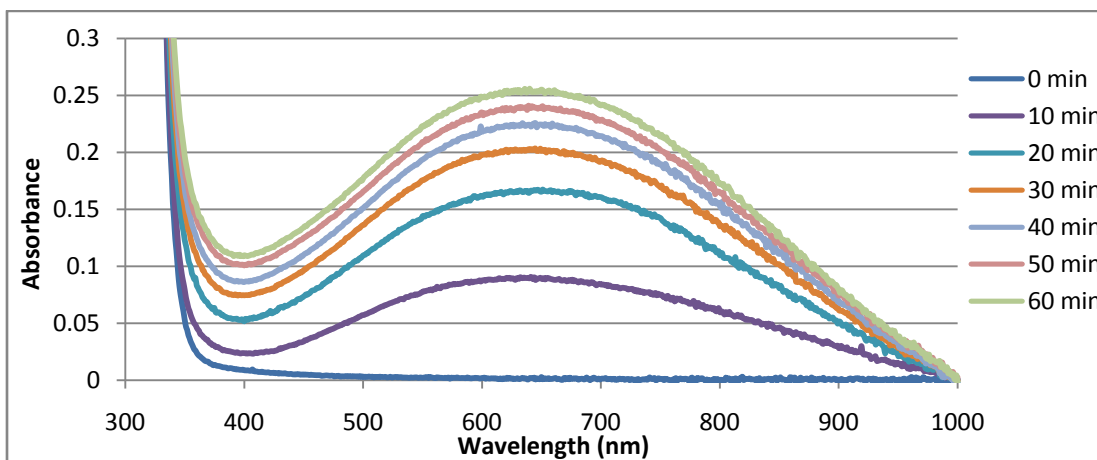


**Figure 5 – Evolution of the Additional Absorption Band in TiO₂ Nanoparticles**

# 4. Semiconductor Nanoparticle and Graphene Oxide Systems

GO-semiconductor nanoparticle systems were obtained through the addition of the solid, graphite oxide powder to a known concentration of nanoparticles in solution. This was followed by sonication of the solution for 30 minutes. The semiconductor nanoparticles naturally adsorb onto the surface of the graphene oxide, and at high nanoparticle concentrations, they completely cover the sheets. The adsorption effect may be attributed to simple Van der Waals or electrostatic forces. A similar effect was witnessed in studies completed with GO and gold nanoparticles [16].

## 4.1. Morphology of Semiconductor-Graphene Oxide Systems

GO-ZnO and GO-TiO$_2$ systems were examined by tapping mode AFM with the Digital Nanoscope III. In this form of microscopy, an atomically-fine silicon tip oscillates over a sample in order to detect changes in sample height as a result of increased or decreased attractive forces between the sample and the tip. This method of microscopy is especially important with respect to graphene and graphene oxide systems, as it can attain vertical resolution on the order of angstroms. The sheet thickness of an individual sheet of graphene is 0.34 nm, whereas graphene oxide sheet thicknesses have dry values of 0.65nm (as determined by X-Ray Diffraction (XRD)) and more-typical values of 1-1.3nm for a hydrated sample examined by AFM [17], [18].

AFM samples were prepared by dropcasting dilute mixtures of the semiconductor nanoparticles and GO sheets in ethanol onto heated, freshly-cleaved mica substrates. Typical AFM images for ZnO and TiO$_2$ nanoparticles anchored to GO sheets are given below in Figure 6 and Figure 7 respectively. The corresponding section-depth profiles of the images are also provided. The ZnO sample is 3:1 ZnO:GO by mass, whereas the TiO$_2$ sample shown is 1:3 TiO$_2$:GO by mass.
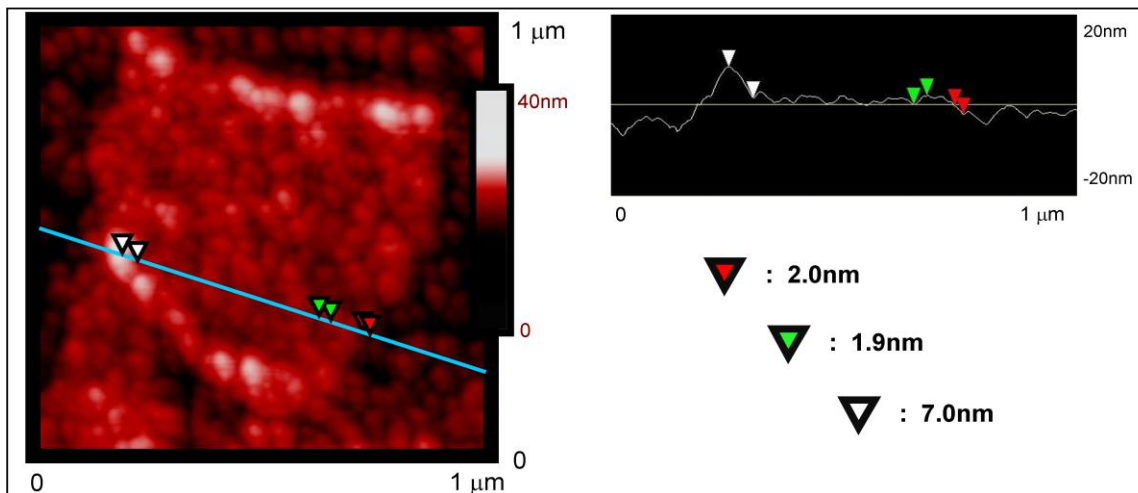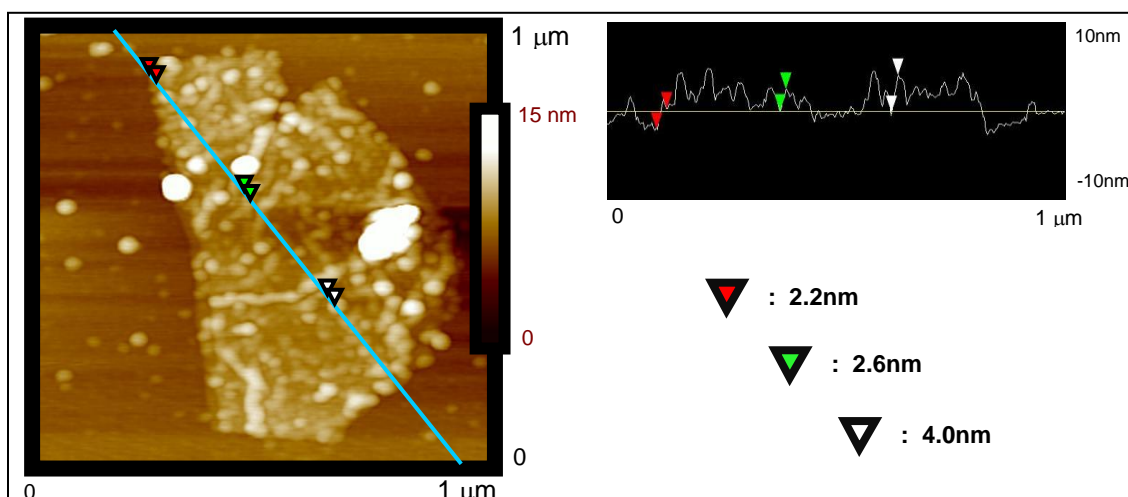


**Figure 6 – AFM Analysis of ZnO Nanoparticles Deposited onto Graphene Oxide Sheets**

7

**Figure 7 – AFM Analysis of TiO$_2$ Nanoparticles Deposited onto Graphene Oxide Sheets**

The GO-ZnO and GO-TiO$_2$ systems are very similar. Both systems consist of nanoparticles on the order of 2-7nm, and the nanoparticles appear to completely cover the graphene sheets. Furthermore, both systems exhibit mono- and bilayer graphene, as indicated by 1-2nm sheet heights. This shows that the exfoliation of graphite oxide by sonication provides disperse and separate sheets. Although we were initially interested in individual graphene sheets, it should be noted that the presence of bilayer and few-layer graphene is not necessarily indicative of poor sample. Studies have shown that bilayer graphene can exhibit conductivities significantly greater than single-layer graphene [5].

## 4.2. Zinc Oxide Nanoparticle Fluorescence Quenching by Graphene Oxide

### 4.2.1. Steady-State Fluorescence Analysis

The ZnO fluorescence shown previously in Figure 4 may be quenched if the absorbed energy can be transferred to another system before the photogenerated electrons and holes recombine. The capacity of ZnO to transfer electrons has been previously explored by the addition of carbon nanotubes to a solution of ZnO nanoparticles [8]. In the present study, it is shown that GO can play a similar role in the quenching of fluorescence of ZnO nanoparticles. Figure 8 below shows the fluorescence of a 1 mM solution of ZnO nanoparticles with varying amounts of graphene oxide added to the solution. Emission spectra were taken using an SLM 8000 photon counting spectrofluorometer at an excitation wavelength of 315nm.

8
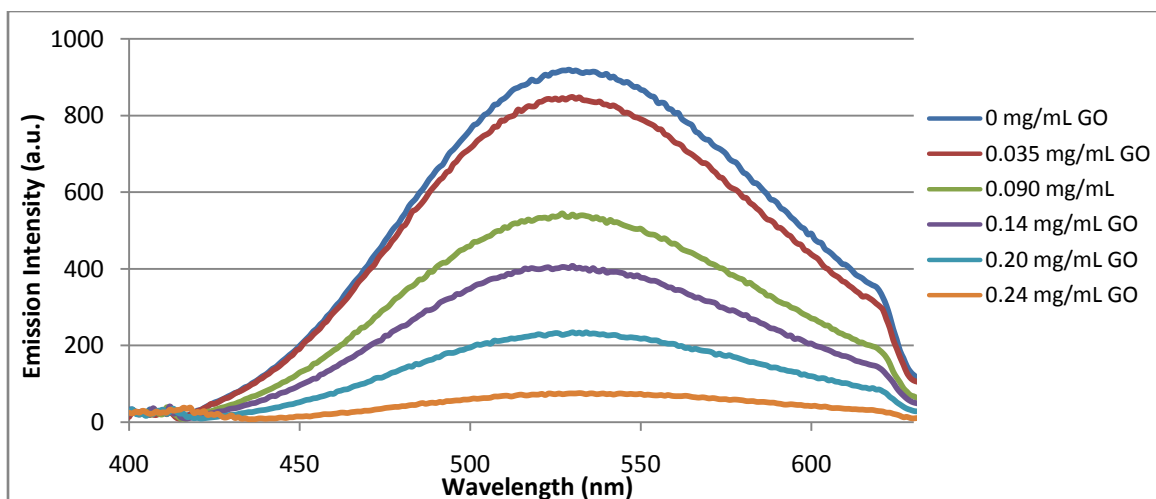
**Figure 8 –Fluorescence of 1 mM ZnO Nanoparticles with Varying Concentrations of GO**

Figure 8 certainly implies that the decrease in fluorescence is indicative of a transfer of energy from the excited ZnO nanoparticles to the GO. However, the presence of GO affects the amount of light that the pure ZnO nanoparticle solution would otherwise absorb. As such, the decrease in fluorescence may simply be a result of the decreased amount of incident radiation striking the ZnO nanoparticles. The absorbance measurements of the above samples are shown below in Figure 9. Samples were placed in 0.5-1cm quartz cells and absorption measurements were taken using a Cary 50 Bio UV-Vis Spectrometer.
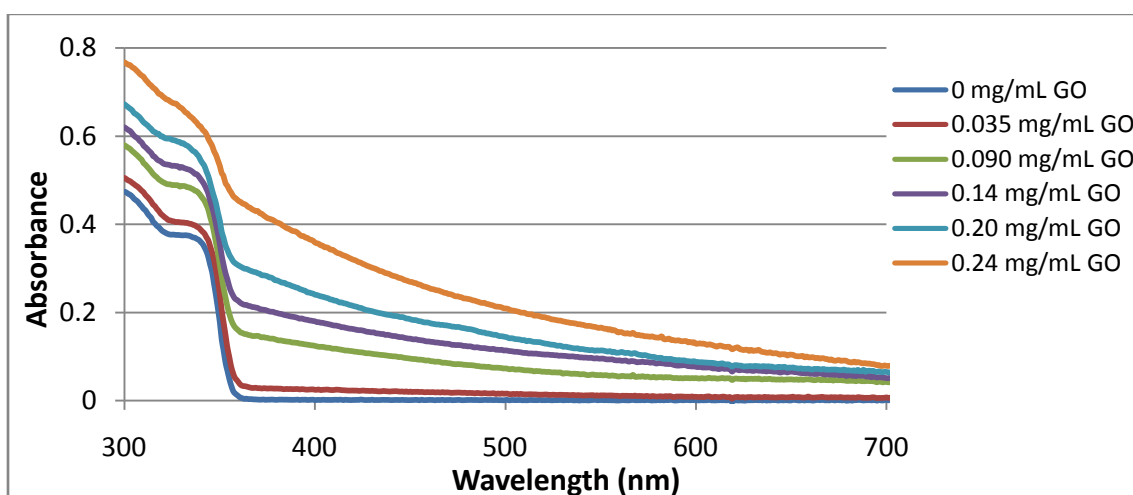


**Figure 9 – Absorption of 1mM ZnO Nanoparticles with Varying Concentrations of GO**

In order to assert a transfer of electrons from the ZnO nanoparticles to GO, it is therefore necessary to prove that the contribution of absorption from graphene oxide is not enough to accommodate for the

significant quenching of ZnO fluorescence. One may derive equation **(2)** in order to calculate the percent of light absorbed for both the pure ZnO nanoparticles and the GO-ZnO solutions.

$$\%Absorbed = \frac{I}{I_0} \cdot 100 = \left(1 - 10^{Absorbance}\right) \cdot 100 \qquad \textbf{(2)}$$

By subtracting the percent absorbed by pure ZnO from the GO-ZnO samples at a specific wavelength, one may find the change in absorption as a result of the GO added to the system. In this study, the specific wavelength is chosen to be 315nm, corresponding to the excitation wavelength previously used to generate the fluorescence in Figure 8. The contribution of GO to the change in absorption can then be calculated as the ratio of the change in absorption to the total absorption. A summary of the calculations for all samples are given in Table 1 below.

**Table 1 – Absorbance Contributions of GO in GO-ZnO Solutions**

|  | Absorbance @ 315 | | % Absorbed | | Change in % Absorbed | % Contribution from GO |
| --- | --- | --- | --- | --- | --- | --- |
| GO (mg/mL) | Pure ZnO | Unreduced | Pure ZnO | Unreduced | | |
| 0.035 | 0.41 | 0.44 | 60.73 | 64.08 | 3.35 | 5.24 |
| 0.09 | 0.41 | 0.51 | 60.73 | 69.39 | 8.67 | 12.49 |
| 0.14 | 0.41 | 0.55 | 60.73 | 72.12 | 11.40 | 15.80 |
| 0.2 | 0.41 | 0.61 | 60.73 | 75.54 | 14.81 | 19.61 |
| 0.24 | 0.41 | 0.71 | 60.73 | 80.52 | 19.80 | 24.59 |

The percent quenching in fluorescence can be calculated as the difference in fluorescence emission counts at the measured peak heights. A summary of calculations for all samples and a comparison of the percent change in absorbance to the percent change in fluorescence are given in Table 2 below. In all samples shown, the change in absorption alone cannot accommodate for the quenching of fluorescence. In the most GO-concentrated sample, the quenching is greater than three times of GO's percent contribution to absorbance. The quenching is therefore believed to be a result of another mechanism: the transfer of electrons to the graphene oxide.

**Table 2 – Fluorescence Quenching of GO-ZnO Solutions**

| Fluorescence @ 530nm | | % Quenching of Fluorescence | % Contribution by Go to Change in Absorption |
| --- | --- | --- | --- |
| Pure ZnO | Unreduced | | |
| 916 | 849 | 7.31 | 5.24 |
| 916 | 542 | 40.83 | 12.49 |
| 916 | 408 | 55.46 | 15.80 |
| 916 | 235 | 74.34 | 19.61 |
| 916 | 75 | 91.81 | 24.59 |

### 4.2.2. Transient Fluorescence Analysis

In order to further substantiate the claims that electrons are transferred from the excited ZnO nanoparticles to the graphene oxide sheets, fluorescence lifetime measurements may be taken on ZnO samples containing various concentrations of GO. In this experiment, pulses of UV radiation are sent to the sample, and the resulting fluorescence decay is measured over a short period of time. The resulting fluorescence can be fit to exponential curves in order to derive time parameters, which can be used to calculate average lifetimes of the fluorescence. Figure 10 below shows the fluorescence decays of a 1mM solution of ZnO nanoparticles with varying concentrations of GO at a monochromator setting of 530nm. Measurements were taken using a Horiba Jobin Yvon single photon counting system with a 277 nm diode with 1 kHz repetition rate and 1.1 ns pulse width. The inset shows the average lifetime as a function of GO concentration.
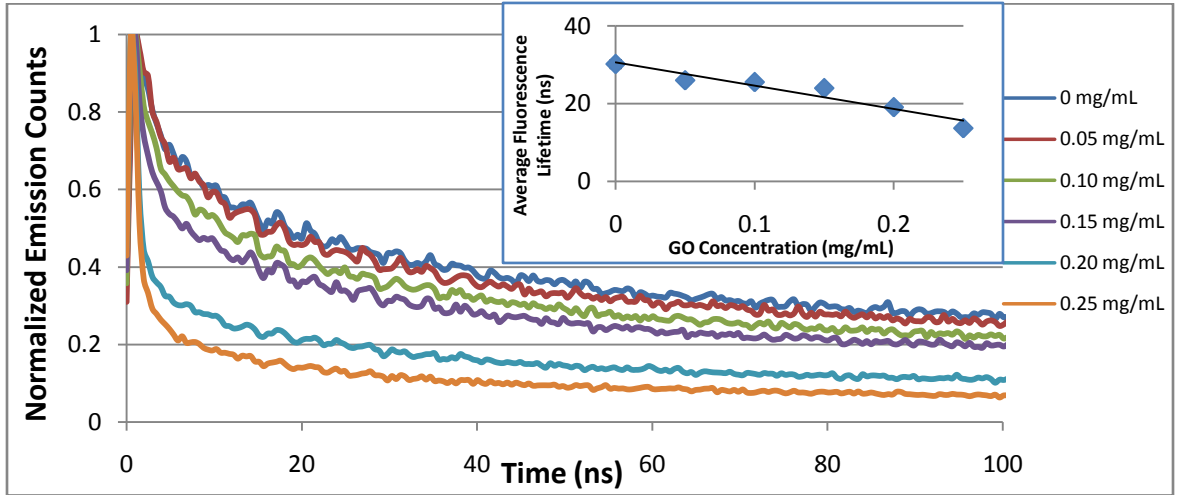


**Figure 10 – Fluorescence Decay Traces of 1mM ZnO with Varying GO Concentrations**

The fluorescence of ZnO nanoparticles exhibits a fast-slow recombination, with the fast component occurring over a 10ns time period, and the slow component decaying over a much longer period of time. Average lifetimes were calculated by fitting the decay traces to biexponential curves in the form of equation **(3)** below over a 100ns time period. The fit parameters were then applied to equation **(4)** below in order to determine the average lifetimes.

$$f(t) = A_1 \cdot e^{-\frac{t}{\tau_1}} + A_2 \cdot e^{-\frac{t}{\tau_2}} \tag{3}$$

$$< \tau > = \frac{\sum_{i=0}^{n} A_i \cdot \tau_i^2}{\sum_{i=0}^{n} A_i \cdot \tau_i} \tag{4}$$

A summary of the calculations and fit parameters are given in Table 3 below. From Figure 10 and Table 3, it is clear that the GO effectively quenches the fluorescence by fast electron transfers from the excited ZnO nanoparticles to the GO. A decrease in average lifetime from 30 to 14ns is observed.

**Table 3 – Average Lifetimes of 1mM ZnO with Varying GO Concentrations**

| GO Concentration (mg/mL) | a1 | t1 (s) | a2 | t2 (s) | t_avg (ns) |
|---|---|---|---|---|---|
| 0 | 0.420 | 2.98E-09 | 0.412 | 3.27E-08 | 30.2 +/- 1.0 |
| 0.05 | 0.434 | 2.84E-09 | 0.423 | 2.84E-08 | 26.0 +/- 0.8 |
| 0.10 | 0.579 | 2.14E-09 | 0.394 | 2.67E-08 | 25.5 +/- 0.6 |
| 0.15 | 0.809 | 1.44E-09 | 0.364 | 2.67E-08 | 24.0 +/- 0.6 |
| 0.20 | 2.09 | 6.76E-10 | 0.235 | 2.37E-08 | 19.1 +/- 0.4 |
| 0.25 | 2.29 | 6.71E-10 | 0.186 | 1.93E-08 | 13.7 +/- 0.3 |

## 5. Reduction of Graphene Oxide by Excitation of Semiconductor Nanoparticles

Several methods have been suggested for the reduction of graphene oxide in order to produce conductive, 2-D layers of graphene. Chemical reduction methods have been previously investigated and have shown to provide positive results, with conductivities only an order of magnitude below that of bulk graphite [5], [7]. Recent endeavours have even allowed for the reduction of graphene oxide in solution by chemical reduction with hydrazine monohydrate, maintaining the disperse sheets through electrostatic repulsions by precise removal of electrolytes [19]. In this section, the photocatalytic reduction of GO by excitation of ZnO and $TiO_2$ nanoparticles has been examined as an alternative method to partially reduce the GO sheets in solution.

### 5.1. Absorption Characterization and Reduction Timeframe

Solutions of GO with ZnO nanoparticles and GO with $TiO_2$ nanoparticles in ethanol were exposed to a 450-W Oriel Xenon Arc Lamp at a current of 9 A. A water filter was used in order to reduce the transmitted infrared radiation to prevent excessive heating of the samples during irradiation. Similar to previous experiments, the solutions were degassed with nitrogen gas for approximately 2 minutes per mL of volume in the reaction vessel. The removal of air from the system is crucial, as oxygen would act as an electron scavenger and hinder or even prevent the transfer of electrons from the excited semiconductor nanoparticles to the GO sheets.

As the solutions were irradiated, they changed in colour from light brown to dark black. Similar colour changes are observed in the chemical reduction of graphene oxide, and it has been suggested that the colour change is indicative of "partial restoration of the [conjugated] π network" in the
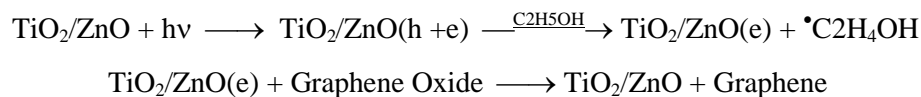
graphene sheets [20]. The colour change can be seen for a GO-ZnO nanoparticle solution in Figure 11 below. The reduced graphene oxide (RGO) was obtained after one hour of irradiation.
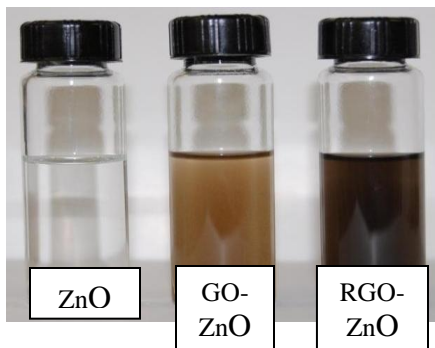


**Figure 11 – Colour Change for a GO-ZnO Nanoparticle Solution after UV Irradiation**

Although the complete reduction mechanism for GO to RGO is unknown, a simple model may be proposed for the transfer of electrons to the GO sheets. UV irradiation of suspensions of $TiO_2$ or ZnO colloids results in charge separation in the semiconducting nanoparticles. The holes are scavenged by ethanol, allowing electrons to accumulate within $TiO_2$ or ZnO nanoparticles. The accumulated electrons serve to interact with the graphene oxide sheets in order to reduce certain functional groups. A reaction scheme for this process is provided below.

$$TiO_2/ZnO + h\nu \longrightarrow TiO_2/ZnO(h + e) \xrightarrow{C2H5OH} TiO_2/ZnO(e) + {}^\bullet C2H_4OH$$

$$TiO_2/ZnO(e) + Graphene\ Oxide \longrightarrow TiO_2/ZnO + Graphene$$

Absorption data for a 1mM ZnO Nanoparticle solution with 0.5mg/mL GO content in a 0.5cm degassing cell are shown in Figure 12 below. The inset shows the absorption change at 460nm over time. The shift in absorption occurs as a result of the darkening of solution, and maximizes after approximately 7 minutes of irradiation. It should be noted that a maximized colour change does not necessarily correspond to a complete reduction – it will be shown in later sections that additional exposure time may result in further reduction.
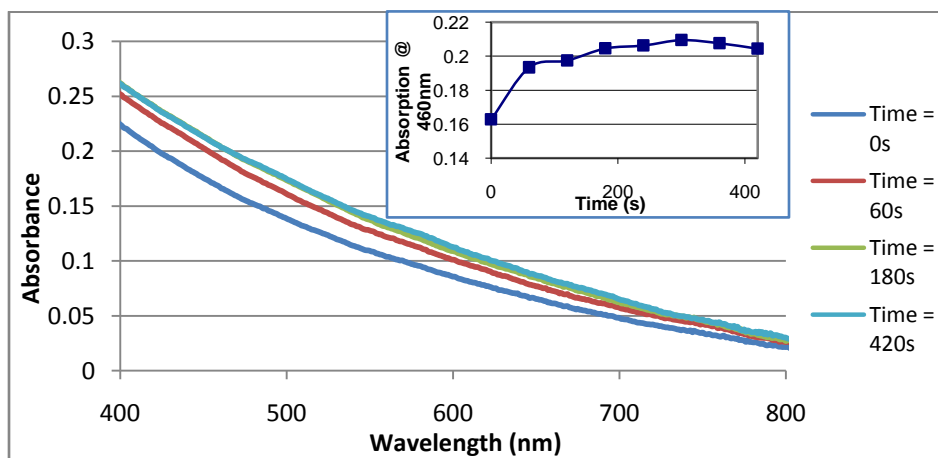


**Figure 12 – Absorption Growth of 0.5 mg/mL GO in 1mM ZnO with UV Irradiation**

13

## 5.2.  Titration of Stored Electrons from $TiO_2$ to Graphene Oxide Sheets

Previous studies with $TiO_2$ colloids have allowed for the determination of the number of trapped electrons corresponding to the growth of the broad absorption band at 650nm.  Through the application of Beer's law, a known amount of $TiO_2$ colloids and a well-researched dye, the molar absorbance of trapped electrons in $TiO_2$ at 650nm was previously determined to be 760 $M^{-1}cm^{-1}$ [9]. As such, the absorption band from $TiO_2$ colloids may be used to quantify the number of electrons transferred to the GO sheets.

In the titration of electrons from $TiO_2$ nanoparticles to GO, 10mM of $TiO_2$ nanoparticles were degassed and placed under UV irradiation for 1 hour until the absorption band at 650nm reached a maximum value.  A separate solution of degassed GO was then added to the $TiO_2$ nanoparticles, resulting in a decrease in the absorption band.  The decrease in the absorption band is indicative of a transfer of the electron to the GO.  In this case, functional groups on the GO are being reduced as the electrons transfer from the $TiO_2$ nanoparticles.  Figure 13 below shows the pre-irradiated $TiO_2$ absorbance as a function of graphene oxide added to the system.
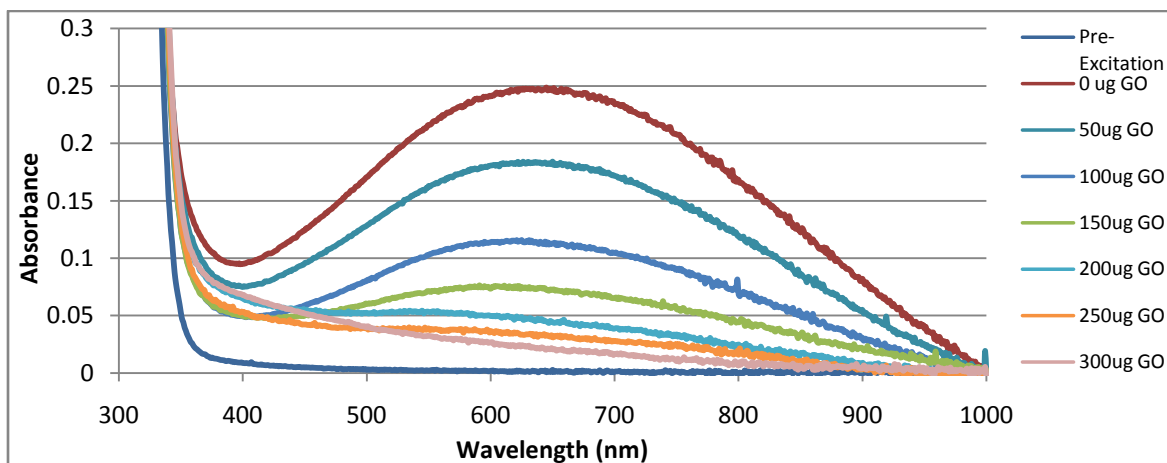


**Figure 13 – Absorption of 10mM UV-Excited $TiO_2$ Colloids with Added GO**

The concentration of trapped electrons corresponding to each absorption trace at 650nm in Figure 13 may be found by applying the Beer-Lambert law as shown in equation **(5)**.

$$Electron\ Concentration = \frac{Absorbance}{\epsilon \cdot l}$$  **(5)**

Using the calculated concentration values, the number of electrons titrated as a function of the mass of GO added to the system can be calculated, as illustrated in Figure 14.
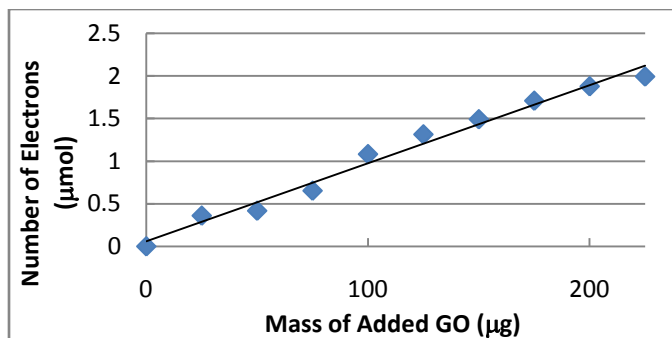
**Figure 14 – Number of TiO$_2$ Electrons Titrated as a Function of Added GO**

The slope of the line in Figure 14 , found to be 0.0092 mol/g, corresponds to the number of electrons consumed per gram of GO.  Using a similar mass composition of the GO as cited in the original preparation of graphitic oxide by Hummers, it is possible to estimate the relative number of oxygen sites that received an electron [11].  A 2.25:1 carbon:oxygen ratio implies 0.019 moles of oxygen per gram of GO.  As such, approximately 50% of the oxygen sites may have potentially received an electron and underwent reduction.

It is important to note that the above calculations do not take into consideration the percentage of transferred electrons that may not have aided in the reduction of GO.  The electron storage capacity of photochemically-reduced graphene oxide was briefly explored by exposing the solution examined in Figure 13 to further irradiation after the addition of GO (corresponding to the complete titration of the initial electrons).   The maximum absorption of the GO-TiO$_2$ nanoparticles was lower than the maximum absorption of the pure TiO$_2$ solution, indicating an equilibrium effect in the storage of electrons between the RGO and the TiO$_2$ nanoparticles.   More specifically, the initial maximum absorption band could not be attained because a fewer number of electrons were trapped in the TiO$_2$ nanoparticles.  This effect is shown in Figure 15 below.  In future research, it is recommended that the storage effect of GO is confirmed and applications of the storage effect are investigated.
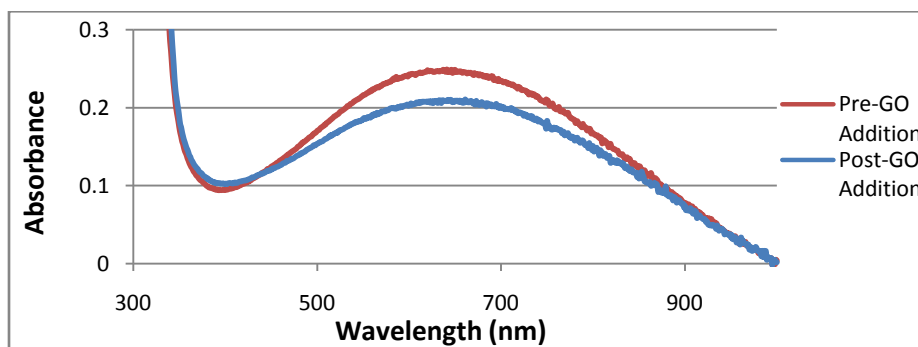


**Figure 15 – Irradiated TiO$_2$ Absorption Band Pre- and Post-GO Addition**

## 5.3. Zinc Oxide Fluorescence Quenching with Reduced Graphene Oxide

Similar studies as those described in section 4.2 were carried out using the RGO samples. The reduced samples were shone under UV light for 1 hour using methods described previously. The reduced samples exhibited even greater fluorescence quenching than the unreduced samples. Comparisons among the steady-state and transient fluorescences of the ZnO nanoparticles with GO prior- and post-reduction are summarized in Table 4 below. The graphs and additional analysis corresponding to this data may be found **Appendix B**.

**Table 4 – Comparison of Fluorescence of Reduced and Unreduced GO-ZnO Samples**

| GO Concentration (mg/mL) | Unreduced Fluorescence Quenching (%) | Reduced Fluorescence Quenching (%) | Unreduced Average Lifetime (ns) | Reduced Average Lifetime (ns) |
|---|---|---|---|---|
| 0.05 | 9.16 | 64.6 | 26.0 +/- 0.8 | 23.6 +/- 0.5 |
| 0.10 | 53.1 | 91.7 | 25.5 +/- 0.6 | 21.1 +/- 0.5 |
| 0.15 | 67.7 | 95.5 | 24.0 +/- 0.6 | 20.1 +/- 0.5 |
| 0.20 | 83.1 | 97.9 | 19.1 +/- 0.4 | 16.3 +/- 0.5 |

The average lifetimes of the ZnO fluorescence decreased by 2 to 4 ns in all samples as a result of the reduction of the GO. Furthermore, the steady-state fluorescence of the samples exhibited a drastic quenching as a result of the reduction, allowing a 90% decrease in fluorescence at only 0.1 mg/mL RGO. The same concentration of GO only allowed a 53% decrease. The above data indicates that the RGO sheets are more conductive and able to accept electrons from the excited semiconductor nanoparticles more readily than their GO counterparts. This effect is desired in the conductive frameworks necessary for sensitized solar cells.

Fluorescence analysis allows one to track the electron as it is first generated and subsequently transferred to the graphene framework. As a further area of research, it may be interesting to couple the GO- and RGO-ZnO nanoparticles with a sensitizing dye in order to further examine the transfer of photogenerated electrons. In this study, the desired electron path would be from the sensitizing molecule to the semiconductor nanoparticle and finally to the GO and RGO sheets. A similar pathway was illustrated earlier in Figure 2.

## 5.4. Resistivity Tests of Graphene Oxide

Solid film resistivity tests were performed as an additional indicator that photocatalytic reduction of GO affects its resistivity. Borosilicate glass coupons were sputtered with a 40-nm layer of gold except for a 2-mm gap in the centre of the coupons. Large resistances between the gold terminations were confirmed before further manipulations to the coupons were made. The GO and RGO solutions were then dropcast on the gap between the gold terminations at slightly elevated temperatures in order to ensure immediate evaporation of the ethanol solvent. The gold terminations were then connected to a Keithley digital multimeter, where resistance measurements of the GO and RGO samples were recorded.

Sheet resistance values were calculated by dividing the measured lateral resistances by the square of the sample (equal to the ratio of the length to the width of the gap). A summary of the results of the resistance measurements are available in Table 5 below.

**Table 5 – Resistances of Unreduced and Photocatalytically Reduced GO**

| | Unreduced GO-ZnO | RGO-ZnO | Unreduced GO-TiO$_2$ | RGO-TiO$_2$ |
|---|---|---|---|---|
| Lateral Resistance (kOhm) | 583 +/- 107 | 16.3 +/- 5.16 | 233 +/- 105 | 30.5 +/- 8.33 |
| Sheet Resistance (kOhm/sq) | 2920 +/- 535 | 81.7 +/- 25.8 | 1170 +/- 525 | 152 +/- 41.6 |

A similar method of determining resistivity changes was previously used for measurements of chemically-reduced graphite oxide [21]. Those measurements found the lateral resistance of a reduced graphite oxide sample across a 2-mm long, 3-mm wide gap to be 12 kOhm, similar to the 16 and 31 kOhm lateral resistance values found for the GO-ZnO and GO-TiO$_2$ samples respectively. However, the unreduced graphite oxide lateral resistance of 32 MOhm is in contrast to the observed values of this experiment. The difference in resistance may be attributed to the conductivity contributions of the semiconductor nanoparticles and differences in film thicknesses.

Large standard deviations were witnessed for all samples. This is believed to be a result of the dropcasting method used in this technique, which provided variations in the quality of films. As such, it is recommended that an additional method of measuring resistivity or conductivity is used to verify the above results and attain more accurate quantitative data. This should aid in the comparison of measured values for the photocatalytically-reduced GO with values for the chemically-reduced GO in literature. A spin-coating approach to achieve a uniform monolayer of GO combined with an evaporated gold deposition technique may provide more-reliable results.

## 5.5.  Thermogravimetric Analysis of GO and RGO

In order to gain a better understanding of the effects of photocatalytic reduction of the GO sheets, Thermogravimetric Analysis (TGA) was performed on solid GO-TiO$_2$ samples prior- and post-reduction.  It should be noted that the two samples were derived from the same solution; however, the RGO sample was exposed to UV light, as described in earlier sections, for 2 hours prior to evaporating the solvent.  In typical GO samples, a slight mass loss due to the storage of water is noticed at 100$^o$C and a significant mass loss is expected at approximately 200$^o$C as a result of the numerous functional groups [18].  Similar effects were witnessed in the GO-TiO$_2$ sample, as shown in Figure 16 below.  The derivatives of the TGA traces were taken to provide a more sensitive measurement of the mass losses.  Furthermore, the contributions of TiO$_2$ to the total masses were subtracted from the measured values before mass percents were calculated.
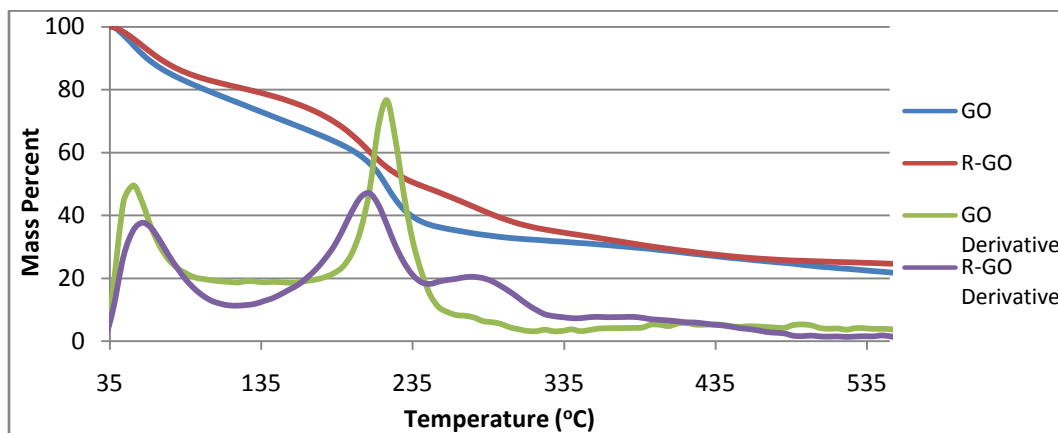


**Figure 16 – Thermogravimetric Analysis of GO and RGO**

The RGO-TiO$_2$ samples exhibited several variations with respect to the unreduced sample.  The mass percent loss at both 100$^o$C and 200$^o$C was smaller than the GO-TiO$_2$ samples indicating a smaller amount of stored water within the graphene sheets and a smaller number of thermally-reducible functional groups.  An even more peculiar observation is the evolution of an additional mass loss at a higher temperature of 250$^o$C.  It is believed that this is due to the reorganization of the functional groups into a more temperature-resistant form.  It is recommended that this effect is further confirmed through a means of functional group analysis, such as Fourier Transform Infrared Spectroscopy.  An important observation from this data is that the photocatalytic reduction of the GO samples does not result in the near-complete loss of the functional groups, as was reported for the chemically-reduced samples previously [18].

18

# 6. Concluding Notes and Further Areas of Research

It has been shown that GO is an effective substrate for the attachment of semiconductor nanoparticles. $TiO_2$ and ZnO nanoparticles both adsorb onto the large 2-D GO sheets naturally through Van der Waals and electrostatic forces. The synthesis and morphology of these systems were studied and provided as a basis of characterization for this report. In order to better understand the GO samples, it is recommended that further studies are made on the synthetic methods used to produce the GO sheets, including analysis on their carbon-to-oxygen ratios, their surface morphology and their suspendability in various solvents. A more definitive approach to the synthesis of graphene oxide would aid in future work and characterization of graphene systems.

The GO-semiconductor nanoparticle systems have unique chemistry that was studied through various photochemical analyses and characterization techniques. In particular, the fluorescence quenching effect of both GO and RGO on ZnO nanoparticles was studied through fluorescence spectrometry and fluorescence lifetime analysis. This analysis provides promising results that graphene sheets may be used in combination with semiconductor nanoparticles as a conductive framework with which to anchor sensitizing molecules or particles.

One of the most challenging aspects of the synthesis of graphene is the separation of graphite into individual sheets. While sonication of GO creates disperse sheets in most polar solvents, GO has poor conductivity compared to bulk graphite, limiting its potential applications in both solar cell research and nanoelectronics. In order to overcome this problem, a method of photocatalytic reduction of the GO sheets was examined, where photoexcitation of semiconductor nanoparticles results in the transfer of electrons and subsequent reduction of oxygen groups on the GO sheets. In order to better characterize this reduction, electron titration experiments were carried out using the unique electron storage capacity of $TiO_2$ nanoparticles. It was found that approximately 50% of the oxygen groups on the GO may potentially receive a stored electron.

Studies were performed on the absorbance change of the GO as it was reduced. A distinct shift in colour from light brown to black was observed during UV-irradiation of the GO-$TiO_2$ and GO-ZnO solutions. Furthermore, TGA of the $TiO_2$-reduced samples was completed, and the electrical resistances of both the GO-$TiO_2$ and GO-ZnO samples (reduced and unreduced) were measured. The resistivity of the reduced samples decreased by an order of magnitude, and the TGA indicated a smaller loss of functional groups at the characteristic temperature of 200-230$^o$C. The TGA of the

19

reduced samples also witnessed the creation of additional mass loss at a higher temperature. This indicates that the photocatalytic reduction mechanism potentially results in the reorganization of functional groups to provide a more temperature-resilient system.

The research described within this report provides a basis and a springboard of opportunities for additional work with graphene and GO systems. In addition to verifying results discussed previously, such as the conductivity changes among the reduced and unreduced systems, and the storage effect of the GO, there are numerous characterization techniques that could be further employed to better-understand the photocatalytic reduction mechanism. NMR was briefly examined as a method of characterization, and showed promising results for functional group analysis of the GO and RGO samples. Additional methods to accomplish this goal may also include Fourier Transform Infrared Spectroscopy (FTIR).

Different GO-semiconductor nanoparticle systems may also be explored to better understand the reduction mechanism. A larger band gap or higher energy semiconductor material may result in even greater reduction of the GO samples. Furthermore, smaller energy band gap semiconductor nanoparticles may aid in the determination of the reduction energy of the functional groups on graphene oxide. Sensitizers may also be coupled with the GO-ZnO and GO-TiO$_2$ nanoparticle systems in order to confirm graphene's role in sensitized solar cells and better understand the electron transfer mechanism. As originally stated, graphene is a relatively unstudied material, especially with respect to photochemistry and solar cell research, so the number of avenues for experimental study and research are nearly limitless.

# References

[1] Kamat, P. V., Bedja, I. and Hotchandani, S., "Photoinduced Charge Transfer between Carbon and Semiconductor Clusters. One-Electron Reduction of C60 in Colloidal Ti02 Semiconductor Suspensions." *The Journal of Physical Chemistry*, Issue 37, Vol. 98, pp. 9137-9142, 1994.

[2] Subramanian, Vaidyanathan, Wolf, Eduardo E. and Kamat, Prashant V., "Green Emission to Probe Photoinduced Charging Events in ZnO-Au Nanoparticles. Charge Distribution and Fermi-Level Equilibration." *The Journal of Physical Chemistry B*, Issue 30, Vol. 107, pp. 7479-7485, 2003.

[3] Ward, Michael D. and Bard, Allen J., "Photocurrent Enhancement via Trapping of Photogenerated Electrons of TiO2 Particles." *The Journal of Physical Chemistry*, Issue 18, Vol. 86, pp. 3599 -3605, 1982.

[4] Bahnneman, D. W., Kormann, C. and Hoffman, M. R., "Preparation and Characterization of Quantum Size Zinc Oxide: A Detailed Spectroscopic Study." *The Journal of Physical Chemistry*, Issue 14, Vol. 91, 1987.

[5] Go´mez-Navarro, C., et al., "Electronic Transport Properties of Individual Chemically Reduced Graphene Oxide Sheets." *Nano Letters*, Issue 11, Vol. 7, pp. 3499-3503, 2007.

[6] Dikin, D. A., et al., "Preparation and Characterization of Graphene Oxide Paper." *Nature*, Vol. 448, pp. 457-460, 2007.

[7] Wang, X., Zhi, L. and Mullen, K., "Transparent, Conductive Graphene Electrodes for Dye-Sensitized Solar Cells." *Nano Letters*, Issue 1, Vol. 8, pp. 323-327, 2008.

[8] Vietmeyer, F., Seger, B. and Kamat, P. V., "Anchoring ZnO Particles on Functionalized Single Wall Carbon Nanotubes. Excited State Interactions and Charge Collection." *Advanced Materials Communications*, Vol. 19, pp. 2935-2940, 2007.

[9] Kongkanand, Anusorn and Kamat, Prashant V., "Electron Storage in SingleWall Carbon Nanotubes. Fermi Level Equilibration in Semiconductor–SWCNT Suspensions." *ACS Nanotechnology*, Issue 1, Vol. 1, pp. 13-21, 2007.

[10] Kamat, P. V., "Meeting the Clean Energy Demand: Nanostructure Architectures for Solar Energy Conversion." *The Journal of Physical Chemistry C*, Issue 7, Vol. 111, pp. 2834-2860, 2007.

[11] Hummers, W. S. and Offeman, R. E., "Preparation of Graphitic Oxide." *The Journal of the American Chemical Society*, Vol. 80, p. 1339, 1958.

[12] Novoselov, K. S., et al., "Two-dimensional atomic crystals." *Proceedings of the National Acadamy of Sciences*. Vol. 102, 2005.

[13] Schniepp, H. C., et al., "Functionalized Single Graphene Sheets Derived from Splitting Graphite Oxide." *The Journal of Physical Chemistry B*, Issue 17, Vol. 110, pp. 8535-8539, 2006.

[14] Worsley, K. A., et al., "Soluble graphene derived from graphite fluoride." *Chemical Physics Letters*, Vol. 445, pp. 51-56, 2007.

[15] Niyogi, S., et al., "Solution Properties of Graphite and Graphene." *Journal of the American Chemical Society*, Issue 24, Vol. 128, pp. 7720-7721, 2006.

[16] Muszynski, Ryan, Seger, Brian and Kamat, Prashant V., "Decorating Graphene Sheets with Gold Nanoparticles." *The Journal of Physical Chemistry C*, Issue 14, Vol. 112, pp. 5263 -5266, 2008.

[17] Schniepp, Hannes C., et al., "Functionalized Single Graphene Sheets Derived from Splitting Graphite Oxide." *The Journal of Physical Chemistry B*, Issue 17, Vol. 110, pp. 8535-8539, 2006.

[18] Stankovich, Sasha, et al., "Synthesis of graphene-based nanosheets via chemical reduction of exfoliated graphite oxide." *Carbon*, Vol. 45, pp. 1558–1565, 2007.

[19] Li, Dan, et al., "Processable aqueous dispersions of graphene nanosheets." *Nature Nanotechnology*, Vol. 3, pp. 101-105, 2008.

[20] Becerril, Héctor A., et al., "Evaluation of Solution-Processed Reduced Graphene Oxide Films as Transparent Conductors." *American Chemical Society Nanotechnology*, Issue 3, Vol. 2, pp. 463-470, 2008.

[21] Kotov, Nicholas A., Dekany, Imre and Fendler, Janos H., "Ultrathin Graphite Oxide-Polyelectrolyte Composites Prepared by Self-Assembly:Transition Between Conductive and Non-Conductive States." *Advanced Materials*, Issue 8, Vol. 8, pp. 637-641, 1996.

# Appendix A: Experimental Procedures

*Graphene Oxide Synthesis*

*Original Preparation Method (used for all experiments described in this report):*

1. Add the following to a reaction vessel kept in an ice bath and stir using a magnetic stir bar:
   - 2g graphite powder
   - 1g sodium nitrate
   - 46mL sulphuric acid
2. Slowly add 6g of potassium permanganate, taking care that the temperature of the solution does not rise above ~20$^o$C
3. Remove the ice bath and bring the temperature up to ~35$^o$C and allow the reaction vessel to sit for 30 minutes to an hour – the solution should become thicker and brownish-gray in colour
4. Add 100mL of water to the reaction vessel slowly and carefully – the temperature of the solution will rise to near 100$^o$C
5. Keep the solution at this elevated temperature (without boiling the solvent) for 15 minutes – the solution should be brown in colour
6. Add 100mL of water with 3% hydrogen peroxide to the reaction vessel
7. Filter the reactants in order to obtain a brown filter cake
8. Wash the filter cake with 1M HCl twice
9. Wash the filter cake with DI water two to three times in order to remove unwanted electrolytes and impurities
10. Scrape the filter cake into an evaporating dish and dry at 60$^o$C for 1 day

*Modified Preparation Method for Better Oxidation:*

1. Add the following to a reaction vessel kept in an ice bath in a sonicator:
   - 200mg graphite powder
   - 200mg sodium nitrate
   - 9.2mL sulphuric acid
2. Sonicate the mixture for 10 minutes while continuously adding ice to the ice bath as it melts
3. Slowly add 1.2g of potassium permanganate to the reaction vessel (while it is sonicated), taking care that the temperature of the solution does not rise above ~20$^o$C
4. Remove the reaction vessel from the sonicator
5. Follow steps 3-10 in the original preparation, using 10 mL and 60 mL of water with 3% hydrogen peroxide for steps 4 and 6 respectively

According to the Hummers' method, the solution should turn yellow upon addition of hydrogen peroxide, indicating a strong oxidation of the graphite powder. In the original formation of graphite oxide, the solution only changed colour to light brown, which was attributed to differences in the graphite powder and variations in volumes of reactants. Using the sonication method, the solution exhibited a bright yellow-orange colour upon addition of hydrogen peroxide.
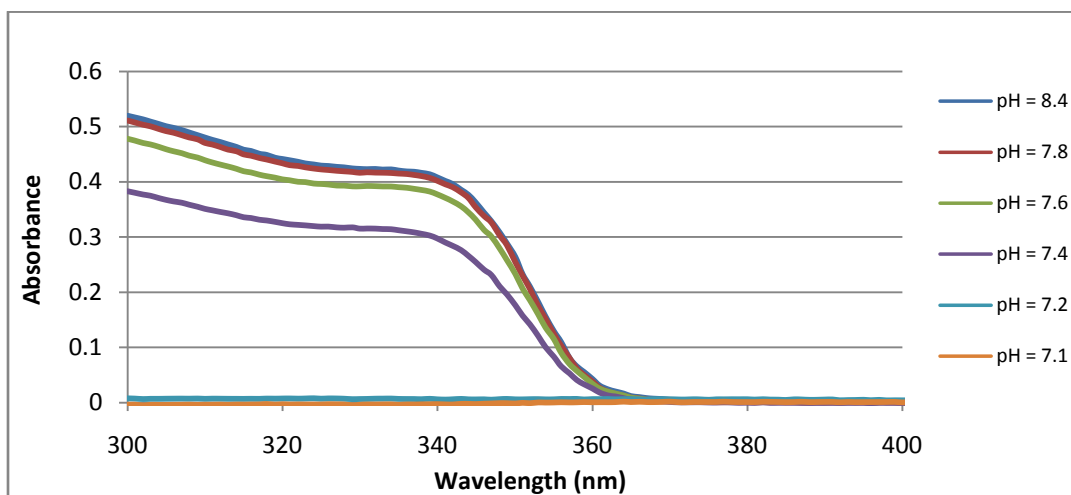
### Zinc Oxide Nanoparticle Synthesis

*Preparation Method:*
1. Add 40 mL of 200-proof ethanol to a capped container (in order to prevent solvent evaporation) and place in an ice bath in a sonicator
2. Allow the solution to cool in the ice bath
3. Add 176mg zinc acetate dihydrate to the reaction vessel while sonicating
4. Sonicate the solution for 5 minutes
5. Remove the ice bath from the sonicator
6. Add 34mg LiOH to the reaction vessel
7. Continue sonicating the solution at room temperature for 5 minutes

This 20mM stock solution of ZnO nanoparticles was further diluted as required for the experiments described in the body of the report. It could be stored for 1-2 weeks before the nanoparticles began to agglomerate and cause the solution to appear cloudy.


*Stability of ZnO Nanoparticles:*
The above reaction was performed in ethanol and in basic conditions in order to promote the formation of Zn-O as opposed to Zn-OH species. The presence of water or an excess of protons in the system causes Zn-OH species to form, resulting in the degradation and eventual loss of the nanoparticles. This behaviour was studied and witnessed by examining the evolution of the ZnO as a function of its pH. Below a pH of 7.4, the unprotected ZnO nanoparticles dissolve into solution, as seen in the **Supplementary Figure 1** below.



**Supplementary Figure 1 – Absorption of 1 mM ZnO Nanoparticles as a Function of pH**

### *Titanium Dioxide Nanoparticle Synthesis*

*Regular Preparation Method:*
1. Add 39.88mL of ethanol to a capped container and keep it stirring vigorously using a magnetic stir bar
2. Slowly (drop-wise) add 0.12mL of reagent-grade titanium isopropoxide to the reaction vessel
3. Wrap the capped container in aluminum foil to prevent the particles from degrading
4. Keep the solution constantly stirring in order to prevent particle agglomeration

The 10mM solution was typically used as prepared and could be kept for several days. After several days or if the solution was not stirred, the solution would turn white in colour, indicating particle agglomeration. In the preparation of $TiO_2$ colloids, it is crucial to use fresh, 200-proof ethanol. The presence of any water in the system will hinder the formation of nanoparticles.

*Acetic-Acid-Stabilized Nanoparticles*:
As an alternative to constant stirring, acetic acid (1-5% by volume) may be added to the ethanol solution in order to stabilize the nanoparticles. It is important to note, however, that the presence of acetic acid results in the creation of an additional absorption band when the $TiO_2$ colloids are shone under UV-light in a deaerated vessel. This band results in a green-coloured solution, instead of the blue solution described in the body of the report. The band does not disappear upon introduction of an electron scavenger to the system, making electron storage calculations impossible.

# Appendix B:  Additional Fluorescence Graphs and Calculations

*Steady-State Fluorescence*

The fluorescence excitation wavelength for all figures below was chosen to be 315nm.  The same wavelength was used for the absorbance calculations below.  The quenching of fluorescence was determined by taking the ratio of maximum fluorescence at 0 mg/mL GO/RGO and the maximum fluorescence at the concentration of interest.
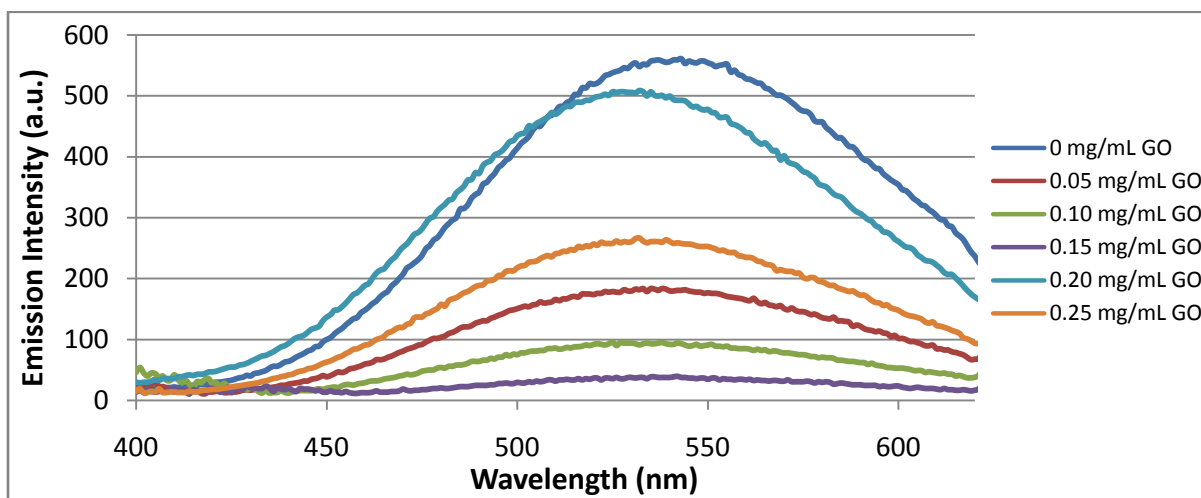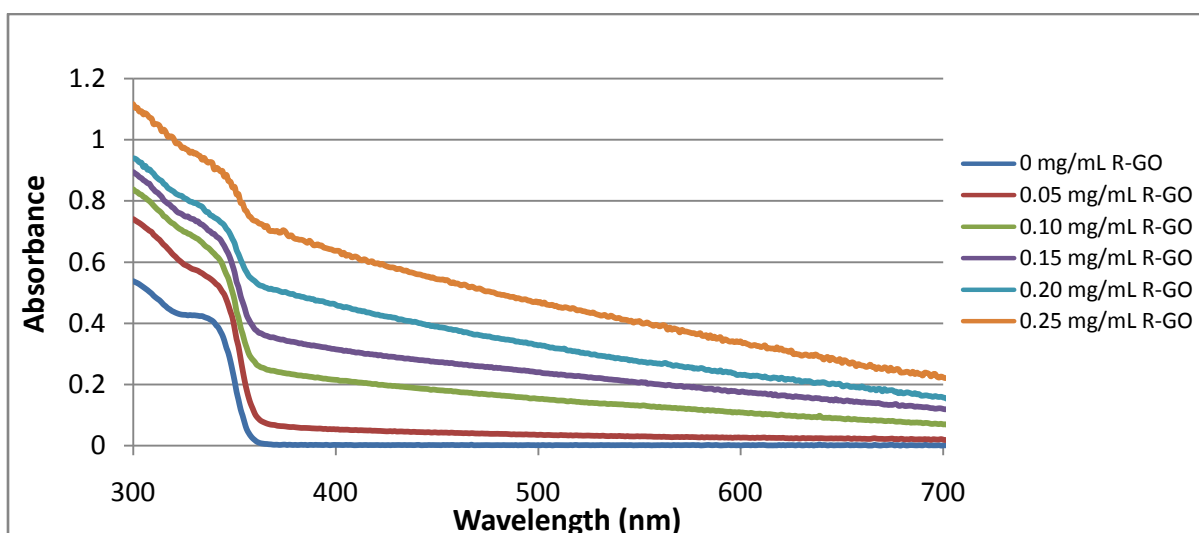


**Supplementary Figure 2 – Fluorescence of 1 mM ZnO Nanoparticles as a Function of GO Concentration**
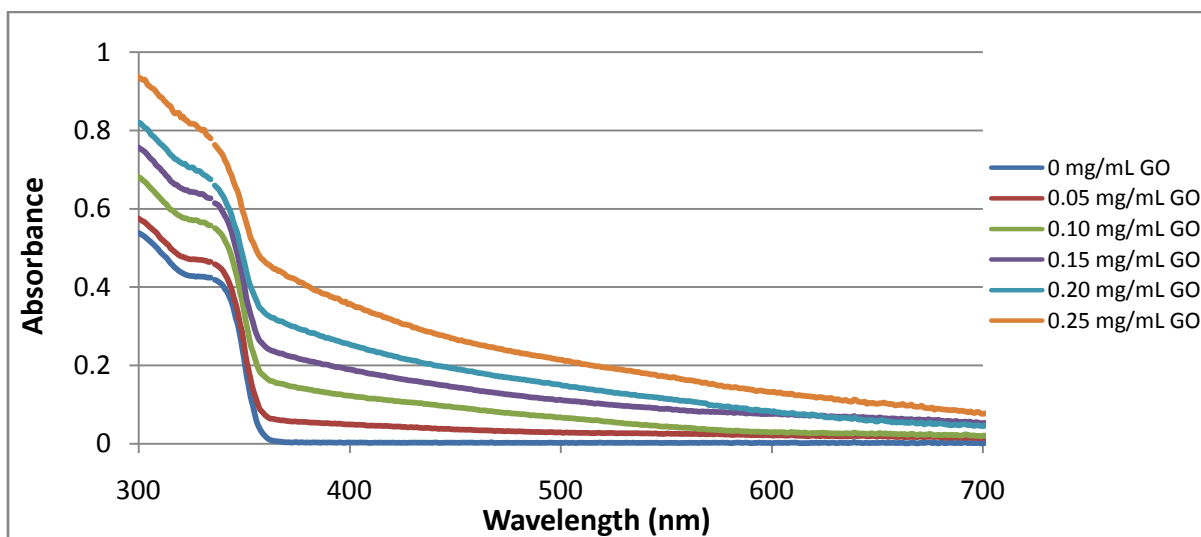


**Supplementary Figure 3 – Absorption of 1 mM ZnO Nanoparticles as a Function of GO Concentration**
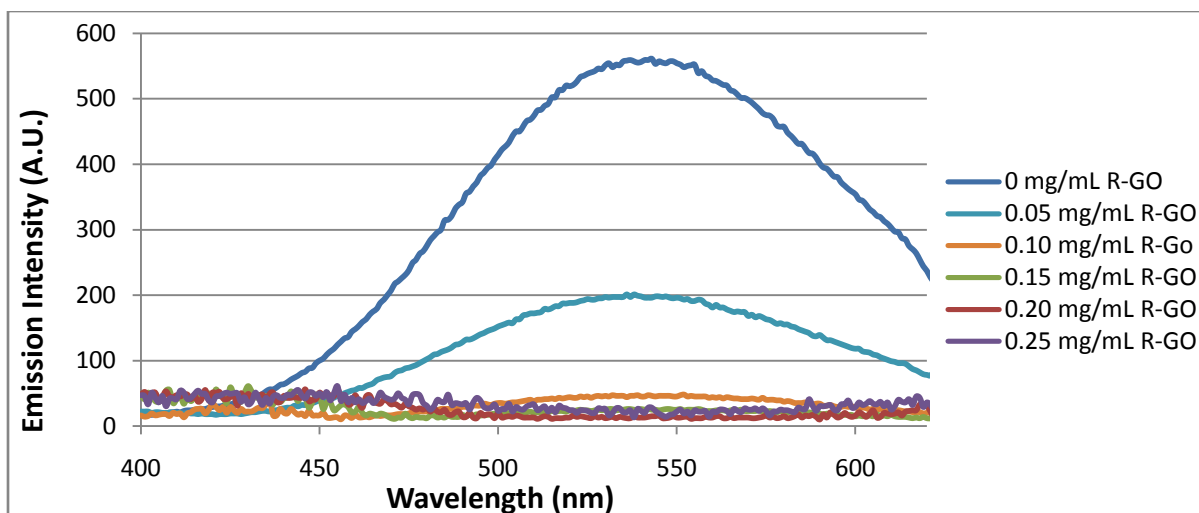
**Supplementary Figure 4 – Fluorescence of 1 mM ZnO Nanoparticles as a Function of R-GO Concentration after 1 hour of UV-Irradiation**



**Supplementary Figure 5 – Absorption of 1 mM ZnO Nanoparticles as a Function of R-GO Concentration after 1 hour of UV-Irradiation**

As shown in the body of the report, calculations must be made to ensure that the addition of GO, or the darkening of GO in the reduction process, cannot accommodate for the significant changes in fluorescence. These calculations are summarized in the following tables.

**Supplementary Table 1 – Change in Absorption vs. Quenching of Fluorescence with Added GO**

| GO (mg/mL) | Change in % Absorbed | % Contribution from GO | % Quenching of Fluorescence |
|---|---|---|---|
| 0.05 | 2.87 | 4.19 | 9.16 |
| 0.10 | 9.30 | 12.44 | 53.14 |
| 0.15 | 13.23 | 16.81 | 67.68 |
| 0.20 | 16.27 | 19.91 | 83.12 |
| 0.25 | 20.81 | 24.12 | 93.18 |

**Supplementary Table 2 – Change in Absorption vs. Quenching of Fluorescence with Added RGO**

| RGO (mg/mL) | Change in % Absorbed | % Contribution from RGO | % Quenching of Fluorescence |
|---|---|---|---|
| 0.05 | 12.55 | 16.09 | 64.63 |
| 0.10 | 16.78 | 20.40 | 91.74 |
| 0.15 | 18.78 | 22.30 | 95.51 |
| 0.20 | 20.61 | 23.95 | 97.85 |
| 0.25 | 25.28 | 27.86 | 95.51 |

**Supplementary Table 3 – Change in Absorption from GO to RGO and Subsequent Additional Quenching of Fluorescence**

| RGO (mg/mL) | Change in % Absorbed | % Contribution from Reduction | % Additional Quenching of Fluorescence |
|---|---|---|---|
| 0.05 | 9.68 | 11.89 | 55.48 |
| 0.10 | 7.48 | 7.97 | 38.60 |
| 0.15 | 5.56 | 5.49 | 27.83 |
| 0.20 | 4.34 | 4.04 | 14.72 |
| 0.25 | 4.47 | 3.74 | 2.33 |

*Transient Fluorescence*
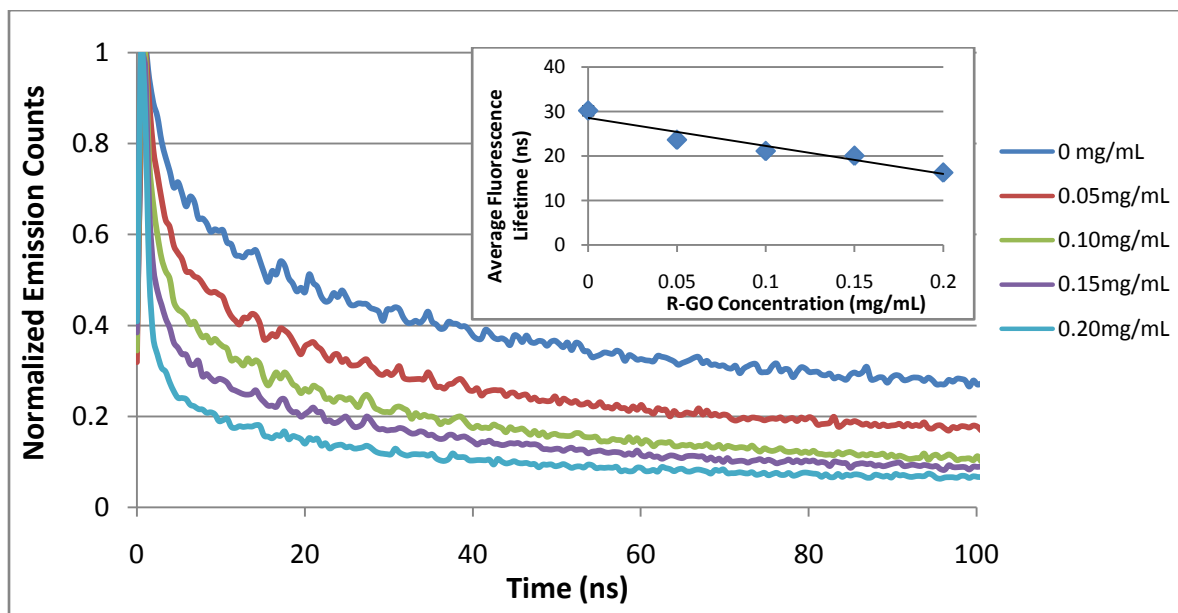


**Supplementary Figure 6 – Transient Fluorescence of 1mM ZnO at Varying RGO Concentrations**

28

The above data was fitted to bioexponential curves. A summary of the fitting data is given in the **Supplementary Table 4** below. Similar calculations as described in the body of the report were used to derive the average lifetimes of the samples.

**Supplementary Table 4 – Average Fluorescence Lifetime of 1mM ZnO at Varying RGO Concentrations**

| RGO Concentration (mg/mL) | a1 | t1 (s) | a2 | t2 (s) | t_avg (ns) |
|---|---|---|---|---|---|
| 0 | 0.420 | 2.98E-09 | 0.412 | 3.27E-08 | 30.2 +/- 1.0 |
| 0.05 | 0.686 | 1.93E-09 | 0.383 | 2.65E-08 | 23.6 +/- 0.5 |
| 0.10 | 1.04 | 1.30E-09 | 0.349 | 2.43E-08 | 21.1 +/- 0.5 |
| 0.15 | 1.46 | 9.98E-10 | 0.276 | 2.42E-08 | 20.1 +/- 0.5 |
| 0.20 | 2.22 | 6.81E-10 | 0.200 | 2.17E-08 | 16.3 +/- 0.5 |